Soft X-Ray Spectrum Unfold of K-Edge–Filtered X-Ray Diode Arrays Using Cubic Splines

D. H. Barnak,[1] J. R. Davies,[1] J. P. Knauer,[1] and P. M. Kozlowski[2]

[1]Laboratory for Laser Energetics, University of Rochester
[2]Los Alamos National Laboratory

Spectrally integrated x-ray diagnostics[1–3] such as the ones fielded at the Omega Laser Facility and the National Ignition Facility make it possible to estimate radiation temperatures and spectral power without the need for crystal spectrometers. An array of x-ray diodes with different K-edge filters samples finite areas of the spectrum in question to determine the radiated power in that band. X-ray mirrors are also used as filters for high-energy photons for K-edge filters at lower-photon-energy bands. The filter components, x-ray diode, cable chain, attenuators, and digitizing oscilloscope form what is commonly referred to as a channel of the array. A typical array of diodes is capable of spanning the soft spectral range from 60 to 3000 eV.

Many methods[4] have been employed in the past to recover the x-ray spectrum from the channel signal traces, some of which require assumptions or measurements for the spectral shape[5,6] or considerations about the geometry[7] of the source. These methods are accurate but can suffer from complications such as insufficient signal-to-noise ratios or lack of signal due to overattenuation, or if the method is used outside of its intended purpose. Several methods have been previously published utilizing B splines[8] for spectral deconvolution,[9,10] along with proposed improvements on such methods utilizing intervals weighted with the relative intensity.[11] Cubic-spline interpolation was also used to obtain unfolded x-ray flux using *a priori* knowledge and several iterations to refine the interpolation.[12] Cubic-spline interpolation provides an alternative analytical way of solving for the temporally and spectrally resolved x-ray flux with no free parameters, assumptions about the geometry, or material of the emitting plasma.

The cubic spline is well known, and several derivations and codes are available as resources.[13–15] Much of the derivation follows the same notation found in Ref. 13 and a brief look at the derivation can be found in Ref. 12. The x-ray flux is interpolated across the entire spectral range with a series of piecewise cubic functions. The boundary of each cubic function lies between the K edges of each channel's response function. The voltages of each diode is then related to the interpolated x-ray flux by

$$V_i = \int_0^\infty \left(\mathbf{M_y} + 3\mathbf{M}_D \boldsymbol{\chi}_1^{-1} \boldsymbol{\chi}_2 \right) \mathbf{y} R_i(E) \Omega_i \, dE, \tag{1}$$

where $\left(\mathbf{M_y} + 3\mathbf{M}_D \boldsymbol{\chi}_1^{-1} \boldsymbol{\chi}_2 \right)$ represents the framework of the cubic function which depends on photon energy, E; $\mathbf{y}$ is the vector of unknown values of the cubic function at the knot points, which are the independent variables for which to solve, and $R_i(E)\Omega_i$ are the response functions and solid angle of the detector of the ith channel. The piecewise function is represented as a matrix to illustrate the linear system of equations that need to be solved in order to complete the reconstruction of the x-ray flux. The unknown values of the spline, $\mathbf{y}$, do not depend on photon energy and therefore do not contribute to the integral. Each row of the matrix is integrated over photon energy, and the matrix is then inverted to find the values of $\mathbf{y}$. Each row of the matrix refers to a channel of the x-ray diode array, and each column represents an interval of the spline. For n channels, there are $n + 1$ unknowns for which to solve; therefore, either the initial value y_1 or the final value y_{n+1} must be arbitrarily specified for the system to be solvable. For the specific implementation shown in this summary, y_1 is calculated by solving for the flat channel contributions similar to previous methods and then using linear interpolation to find the value of y_1. Ultimately, the cubic spline solution is insensitive to the value chosen for y_1 as shown in Fig. 1.
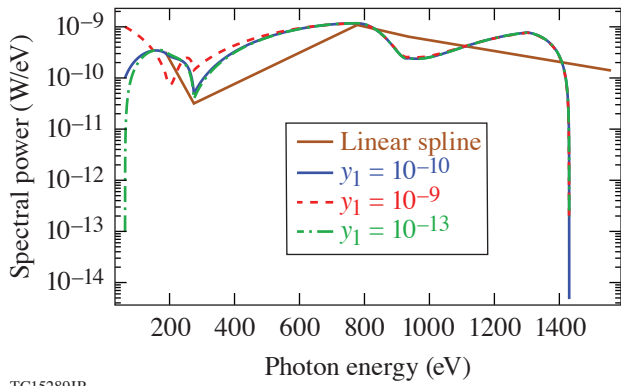
TC15289JR

Figure 1
The initial estimate of the first knot point value of the spline is the only part of the spline that is arbitrary. However, a linear spline calculation that can be solved with no free parameters can provide a good estimate of the initial value of the spline and thereby eliminate this free parameter. In the case where $y_1 = 10^{-9}$, even a slight overestimation of the spectral power can have a drastic impact and can even break the spline by giving non-physical results. The case inspired by the linear spline solution, $y_1 = 10^{-10}$, is equivalent to a gross underestimation of the initial value, $y_1 = 10^{-13}$.

Two sources of possible error propagate from measurement uncertainty: (1) measurement and calibration of the response functions[16] of each channel in the array; and (2) uncertainty and variation in the signal voltages digitized on the oscilloscope. Since the cubic spline is solved exactly from these quantities, an analytical expression for the uncertainty of the spline can be obtained. Each element of the matrix $\int_0^\infty \left(\mathbf{M_y} + 3\mathbf{M}_D \chi_1^{-1} \chi_2 \right) R_i(E) \Omega_i dE$ has an associated error from the response functions. Matrix inversion operations compound these error covariances enough to make even small covariances matter in the calculation. Finding an analytical solution in simple cases like a 2×2 matrix is easy, but it still differs from the results calculated via Monte Carlo when errors cause the matrix to be close to singular.[17] Therefore, error propagation for matrix inversion must be done via Monte Carlo.

After the Monte Carlo error propagation, all of the error analysis can be done analytically. The error for all y_i values can be calculated from the matrix inverse $\mathbf{S}$:

$$\sigma_{y_i} = \left\{ \sum_j \left(S_{i,j} V_j \right)^2 \left[\left(\frac{\sigma_{S_{i,j}}}{S_{i,j}} \right)^2 + \left(\frac{\sigma_{V_j}}{V_j} \right)^2 \right] \right\}^{1/2}, \tag{2}$$

where $S_{i,j}$ is an element of the matrix inverse, $\sigma_{S_{i,j}}$ is the associated error of that matrix element calculated via Monte Carlo, and σ_{V_j} is the random error associated with the measured voltage V_j of the jth channel. From here the rest of the cubic spline error can be calculated analytically.

A simple blackbody model and a detailed atomic model demonstrate how accurately cubic-spline interpolation recovers the temporally and spectrally resolved x-ray flux. A sample radiation temperature curve was used to generate synthetic diode voltage traces by convolving the blackbody spectrum with the channel response functions. These synthetic voltage traces were then used as input to the cubic-spline interpolation, and the solutions are then compared to the inputs as in Fig. 2. The cubic spline is able to solve for the blackbody spectrum and the radiation temperature accurately.

A detailed atomic model of a CNOFNe plasma was also used as an input to the cubic-spline interpolation to test the capability of the method to resolve an x-ray flux that is dominated by line emission (see Fig. 3). The input x-ray spectrum is compared visually to the output of the cubic-spline interpolation, and the spectral power in three different sections of the spectrum is compared numerically. The worst part of the spectrum overestimates the spectral power by a factor of 2, whereas the other two parts of the spectrum recover the spectral power exactly. Overall, the systematic error in the spectral power from the entire unfold is 20% from the cubic spline's inability to resolve the line structure, which corresponds to a 5% error in the radiation temperature. The systematic error is much smaller than the error that stems from the combination of the random error in the voltage trace and the error in measuring the response function in this case, so the conclusion is that the cubic-spline method can adequately recover line-dominated spectra.
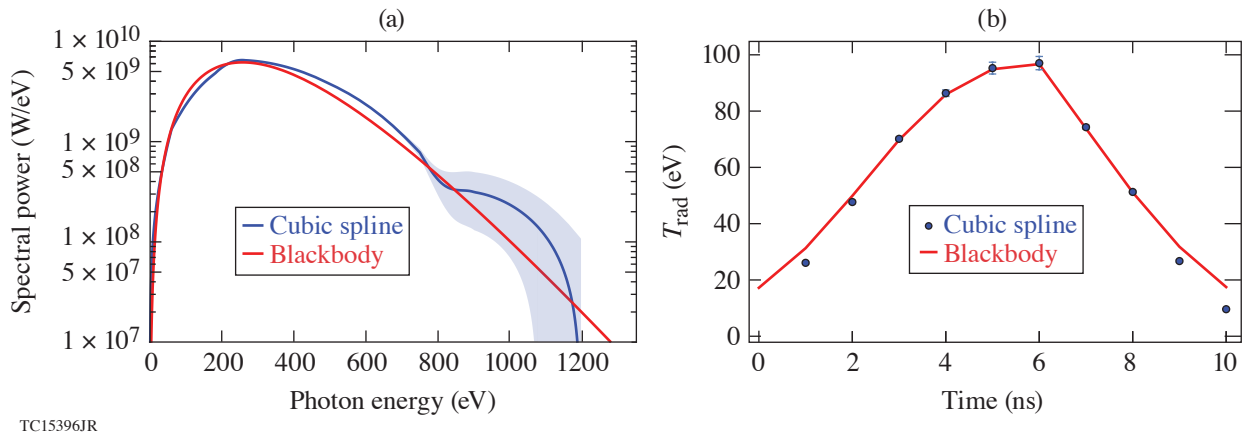
TC15396JR

Figure 2

(a) The cubic spline is able to accurately reconstruct the blackbody spectrum at peak radiation flux. The shaded region around the spline solution represents a typical error associated with calibrated response functions. (b) The input radiation temperature curve used to generate the blackbody spectra and synthetic voltage traces plotted with the radiation temperature solution of the cubic spline at every nanosecond.
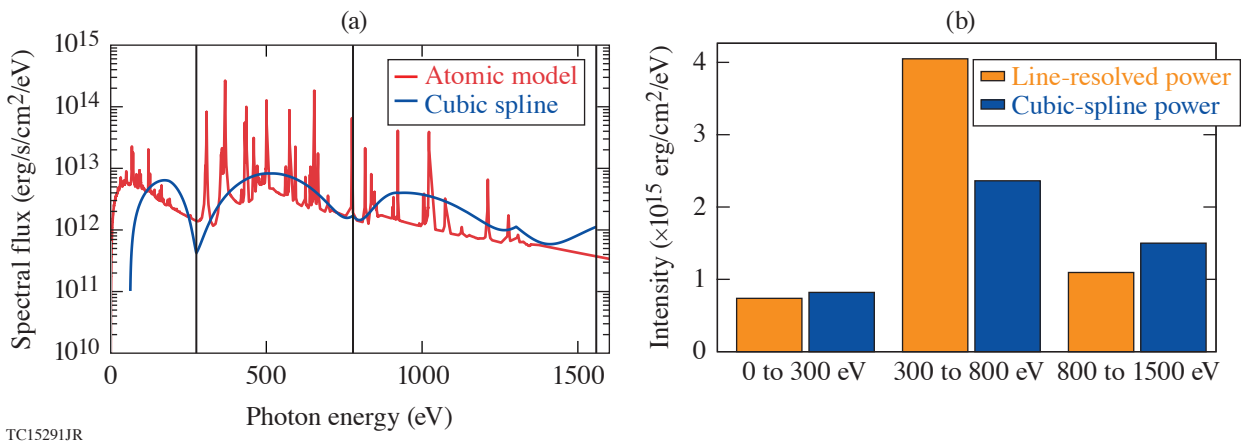

TC15291JR

Figure 3

An atomic model of a CNOFNe plasma is convolved with the channel response functions. The resulting numbers are then used as signal inputs to the cubic-spline unfold algorithm. (a) The recovered cubic-spline spectrum is compared graphically to the atomic model. (b) The spectrum is divided into three line groups, and the integrated intensity of each line group is compared between the atomic model and the cubic spline. The cubic spline is able to conserve spectral power to within a factor of 2 or better in cases where the emission is extremely line dominated.

1. J. L. Bourgade *et al.*, Rev. Sci. Instrum. **72**, 1173 (2001).

2. E. L. Dewald *et al.*, Rev. Sci. Instrum. **75**, 3759 (2004).

3. C. Sorce *et al.*, Rev. Sci. Instrum. **77**, 10E518 (2006).

4. A. Seifter and G. A. Kyrala, Rev. Sci. Instrum. **79**, 10F323 (2008).

5. R. E. Marrs *et al.*, Rev. Sci. Instrum. **86**, 103511 (2015).

6. M. J. May *et al.*, Rev. Sci. Instrum. **87**, 11E330 (2016).

7. M. J. May *et al.*, Rev. Sci. Instrum. **83**, 10E117 (2012).

8. R. Goldman, Pyramid Algorithms: *A Dynamic Programming Approach to Curves and Surfaces for Geometric Modeling*, 1st ed. (Elsevier, Paris, 2003), pp. 347–443.

9. J. Li *et al.*, Rev. Sci. Instrum. **80**, 063106 (2009).

10. D. L. Fehl *et al.*, Rev. Sci. Instrum. **71**, 3072 (2000).

11. S. Tianming, Y. Jiamin, and Y. Rongqing, Rev. Sci. Instrum. **83**, 113102 (2012).

12 J. P. Knauer and N. C. Gindele, Rev. Sci. Instrum. **75**, 3714 (2004).

13. R. H. Bartels, J. C. Beatty, and B. A. Barsky, *An Introduction to Splines for Use in Computer Graphics and Geometric Modeling*, 1st ed. (Morgan Kaufmann Publishers, San Mateo, CA, 1987), pp. 9–17.

14. R. L. Burden and J. D. Faires, *Numerical Analysis*, 6th ed. (Brooks/Cole, Pacific Grove, CA, 1998), pp. 120–121.

15. W. H. Press *et al.*, *Numerical Recipes in FORTRAN: The Art of Scientific Computing*, 2nd ed. (Cambridge University Press, Cambridge, England, 1992), pp. 107–110.

16. K. M. Campbell *et al.*, Rev. Sci. Instrum. **75**, 3768 (2004).

17. M. Lefebvre *et al.*, Nucl. Instrum. Methods Phys. Res. A **451**, 520 (2000).